Magneto-Optical Kerr Effects of Yttrium-Iron Garnet Thin Films Incorporating Gold Nanoparticles

Satoshi Tomita*
PRESTO, Japan Science and Technology Agency (JST), Wako, Saitama 351-0198, Japan

Takeshi Kato and Shigeru Tsunashima
Department of Electronics, Nagoya University, Chikusa, Nagoya 464-8603, Japan

Satoshi Iwata
Center for Cooperative Research in Advanced Science and Technology, Nagoya University, Chikusa, Nagoya 464-8603, Japan

Minoru Fujii and Shinji Hayashi
Department of Electrical and Electronics Engineering, Kobe University, Nada, Kobe 657-8501, Japan
(Received 6 September 2005; published 28 April 2006)

We report an experimental study on magneto-optical (MO) Kerr effects of yttrium-iron garnet (YIG) thin films incorporating Au nanoparticles. The polar MO Kerr spectra in the wavelength between 400 and 800 nm show that, by incorporating the Au nanoparticles, Kerr rotation angles become negative values in the region, where the localized surface plasmon polariton (SPP) resonance of the Au nanoparticles is located. The anomalous Kerr rotation indicates a possible coupling between the MO Kerr effect of YIG and the SPP. A mechanism for the coupling is discussed.

DOI: 10.1103/PhysRevLett.96.167402 PACS numbers: 78.67.Bf, 73.20.Mf, 78.20.Ls

The surface plasmon polariton (SPP) is a coupled mode of electromagnetic waves and collective oscillations of free electrons in nanostructures of noble-metal, which is accompanied by an optical near-field [1]. Manipulating the near-field and enhancing a local field in nanostructured materials are now central problems of the growing field of plasmonics that is of importance for surface-enhanced Raman scattering (SERS) [2], electromagnetic waveguide [3], and subwavelength lithography [4]. When the nobel-metal nanostructures are embedded in a magneto-optical (MO) medium, it is expected that the SPP of the nanostructures is coupled to the MO effects of the medium, leading to a modification and enhancement of the MO properties; this might be considered as a MO counterpart of SERS [5].

Coupling between MO effects and bulk plasma of charge carriers in metals was initially investigated by Feil and Haas [6] and by Katayama *et al.* [7] Safarov and co-workers [8] studied a MO Kerr property of Au/Co/Au multilayer structures in total reflection geometry, and demonstrated a strong enhancement of the MO figure of merit of the system. This indicates that the traveling SPP generated in the Au layers successfully coupled to the MO effect of the Co layer via an evanescent field. Such surface-enhanced MO effects in multilayer systems have been studied intensively owing to their potential application for MO media [9–12]. On the other hand, little is known about a MO effect coupled with the localized SPP of noble-metal nanoparticles via an optical near-field, although such a kind of contribution has been theoretically predicted [5,13].

Let us assume a MO-active medium containing noble-metal nanoparticles, which are MO inactive. Owing to the large specific surface of the nanoparticles, a small volume fraction of the particles effectively influences MO properties of the surrounding medium. In contrast to the SPP on planer metal surfaces, the localized SPP of the nanoparticles can be excited directly by the traveling light wave. A frequency of the SPP depends on the size, shape, and arrangement of the nanoparticles, as well as the kinds of metal. This results in a tailored SPP resonance located in a wide range from visible to near infrared. Moreover, the penetration length of the near field by the localized SPP depends not on the wavelength of the incident light but on the size of nanoparticles. These enable us to study how the near-field contribution influences the MO properties and to provide an insight into the physics underlying in the coupling between the localized SPP and MO effects.

Ferrimagnetic $Y_3Fe_5O_{12}$ (yttrium-iron garnet: YIG) is a well-known insulating MO medium, which is almost transparent in the visible region above 500 nm [14]. In this Letter, we have prepared YIG thin films incorporating Au nanoparticles, the localized surface plasmon resonance of which is located at about 600 nm. Polar MO Kerr effects of the films were studied in the visible region. It was found that, by incorporating the Au nanoparticles, the Kerr rotation angles at about 600 nm show negative values, indicating a possible coupling between the MO effect of YIG and the SPP of Au nanoparticles. The present study opens a way to the near-field optomagnetics in nanocomposite materials.

Thin films consisting of metallic Au nanoparticles embedded in crystalline YIG matrices were prepared through the cosputtering method together with thermal annealing [15]. Au and YIG targets were simultaneously sputtered in an Ar gas atmosphere (20 m Torr) using an rf-sputtering apparatus; the mixture of Au and YIG was deposited onto quartz substrates. The volume fraction of Au in the films (v_{Au}) was evaluated through electron-probe microanalyses. In the present work, we focus on three films with $v_{\mathrm{Au}} = 0\%$, 1.7%, and 10.9%. Thickness of the films were about 500 nm for the $v_{\mathrm{Au}} = 0\%$, 1.7% samples and about 200 nm for the $v_{\mathrm{Au}} = 10.9\%$ sample. All the films were annealed in N_2 gas at 900 °C.

Figure 1(a) shows x-ray diffraction (XRD) profiles of the films. A Cu Kα radiation ($\lambda_{\mathrm{CuK}\alpha} = 1.54$ Å) was used. An XRD profile of a film without Au, i.e., $v_{\mathrm{Au}} = 0\%$, is consistent with that of YIG having the garnet structure. This suggests that deposited YIG is crystallized and a polycrystalline YIG film is formed by annealing at 900 °C. An XRD profile of a film with $v_{\mathrm{Au}} = 1.7\%$ exhibits diffraction peaks, whose positions agree with those of polycrystalline YIG film. However, it shows no traces of Au. This is probably caused by the low volume fraction of Au in the film. In a profile of a film with $v_{\mathrm{Au}} = 10.9\%$, five diffraction peaks assigned to fcc Au emerge in addition to weak signals corresponding to YIG, demonstrating that metallic Au is grown and crystalline YIG and Au coexist in the film.

A cross section of the films was observed with a transmission electron microscope (TEM) operated at 200 kV. The specimens for the TEM observations were prepared through standard procedures including mechanical and Ar-ion thinning techniques. Figure 1(b) shows a cross-sectional TEM image of a film with $v_{\mathrm{Au}} = 10.9\%$. We see that spherical particles are embedded randomly in the film. These are most likely Au nanoparticles. The average diameter of the Au nanoparticles observed was about 12.3 nm. The XRD and TEM studies allow us to depict that, in a film with $v_{\mathrm{Au}} = 10.9\%$, spherical metallic Au nanoparticles about 12 nm in diameter are embedded in the crystalline YIG matrices.

Figure 2 shows UV-Vis transmission spectra for the films in wavelength (λ) ranging from 190 to 2000 nm. The spectra were obtained with a double-beam-type spectrometer. A YIG film with $v_{\mathrm{Au}} = 0\%$ (dash-dotted curve) shows strong absorption below 500 nm corresponding to a charge transfer (CT) type electron transition in YIG [16]. Contrastingly, the film is almost transparent above 500 nm even though there are weak dips at 620 nm and 1000 nm caused by interference. Incorporation of Au with $v_{\mathrm{Au}} = 1.7\%$ (dashed curve) results in strong absorption at about $\lambda = 600$ nm. In a spherical small inclusion with a dielectric function $\epsilon_i(\lambda)$ embedded into a medium with $\epsilon_m(\lambda)$, a surface mode (Fröhlich mode) is excited at λ_F, where $\mathrm{Re}[\epsilon_i(\lambda_F)] = -2\,\mathrm{Re}[\epsilon_m(\lambda_F)]$ is satisfied [17]. If we adopt a dielectric function of Au [18] to $\epsilon_i(\lambda)$ and that of YIG [14] to $\epsilon_m(\lambda)$, λ_F is calculated to be about 600 nm. Therefore, the strong absorption originates from the localized SPP of Au nanoparticles in YIG matrices. This indicates that a film with $v_{\mathrm{Au}} = 1.7\%$ contains metallic Au nanoparticles, which are similar to those in a film with $v_{\mathrm{Au}} = 10.9\%$, although an XRD profile shows no traces of Au. The absorption at about 600 nm becomes stronger with increasing v_{Au} up to 10.9% as shown by a solid curve.

The polar MO Kerr effect at room temperature was studied in λ ranging from 400 to 800 nm using a polarization plane modulation technique with a Faraday cell. The resolution of the Kerr rotation angle was about 0.001°. A Xe lamp was used for the light source. The monochromatic light was illuminated on a film under the magnetic field applied up to ±15 kOe in perpendicular direction to the film plane. The Kerr angle was determined from a rotation angle at about 3 kOe because magnetization hysteresis curves obtained with a superconducting quantum interfer-

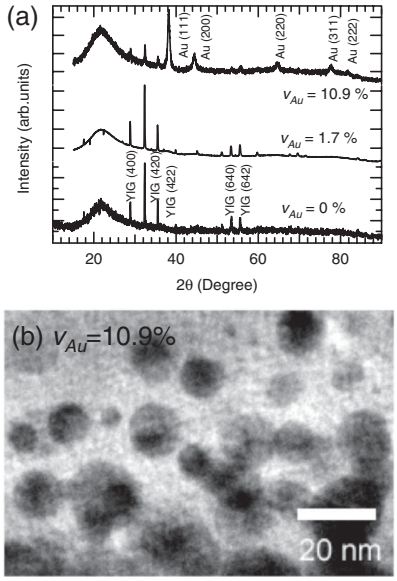

FIG. 1. (a) XRD profiles for films with $v_{\mathrm{Au}} = 0\%$, 1.7%, and 10.9% annealed at 900 °C. (b) A cross-sectional TEM image of a film with $v_{\mathrm{Au}} = 10.9\%$.

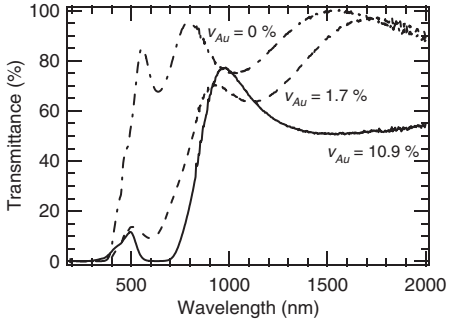

FIG. 2. UV-Vis transmission spectra of films with $v_{\mathrm{Au}} = 0\%$ (dash-dotted curve), 1.7% (dashed curve), and 10.9% (solid curve).

ence device magnetometer (not shown here) indicated that the film magnetization was saturated at about 3 kOe.

Figure 3 shows the Kerr spectra of the samples with $v_{\mathrm{Au}} = 0\%$ (crosses), 1.7% (triangles), and 10.9% (circles). For a YIG film ($v_{\mathrm{Au}} = 0\%$), we see a large Kerr rotation and strong oscillation of the spectrum at about 450 nm, which is probably due to a CT transition at $\lambda = 490$ nm in YIG. Above $\lambda = 500$ nm, although the Kerr angle still oscillates, it remains positive values between 0.07° and 0.01°. This is thought to be caused by a tail of the CT transition. For the $v_{\mathrm{Au}} = 1.7\%$ sample, the Kerr spectra below $\lambda = 500$ nm is similar to that for $v_{\mathrm{Au}} = 0\%$. Contrastingly, the spectrum above 500 nm is much different from the control spectrum. In particular, it should be noted here that the Kerr rotation in the $v_{\mathrm{Au}} = 1.7\%$ sample changes the sign at $\lambda = 530$ nm and the rotation angles become negative values in λ ranging between 540–600 nm. As v_{Au} increases up to 10.9%, the negative Kerr angle appears in a wider range of λ from 520 to 710 nm although the oscillation below $\lambda = 500$ nm is smeared out.

Figure 4 shows the Kerr loops between ±15 kOe obtained for the $v_{\mathrm{Au}} = 10.9\%$ sample. In Fig. 4(a), the loop at $\lambda = 400$ nm exhibits a positive Kerr angle of about 0.04° at 3 kOe. On the other hand, the Kerr loop at $\lambda = 650$ nm [Fig. 4(b)] shows a negative Kerr angle about −0.01° although the value is relatively small. These results verify that the polarization plane of the incident light rotates into the opposite direction between 400 and 650 nm in the $v_{\mathrm{Au}} = 10.9\%$ sample.

In Fig. 3, the absorption spectra converted from the transmission spectra in Fig. 2 are also exhibited. The absorbance at λ [$A(\lambda)$] was calculated through an equation, $A(\lambda) = -\log_{10}[T(\lambda)/100]$, where $T(\lambda)$ is the transmittance at λ. The localized SPP in Au nanoparticles is excited in the vicinity of 602 nm for the $v_{\mathrm{Au}} = 1.7\%$ sample and of 634 nm for the $v_{\mathrm{Au}} = 10.9\%$ sample. An increase in v_{Au} leads to a redshift of the SPP absorption peak [19]. It should be noticed here that the position of the absorption peaks due to the SPP excitation is consistent with the region, where the Kerr rotation angles become negative values. A redshift of the absorption peak for $v_{\mathrm{Au}} = 10.9\%$ brings about the negative Kerr rotation angle at a longer wavelength up to 710 nm. These point out a possible coupling between the MO Kerr effects of YIG and the localized SPP of Au nanoparticles.

The angle of the polar MO Kerr rotation is phenomenologically determined by both the diagonal (ϵ_{xx}) and off-diagonal part (ϵ_{xy}) of electric permittivity. The ϵ_{xx} of the films is modified by incorporating Au into YIG films and forming the composite. It is, however, unlikely that only such a modification causes the negative Kerr rotation in the region of 600 nm even if the multiple refraction is taken into consideration. The incorporation of Au nanoparticles and excitation of the SPP is thus thought to modify ϵ_{xy} of the films [13].

From the microscopic point of view, ϵ_{xy} is related to the electron transition energy, oscillator strength of the transition, and spin-orbit (SO) splitting of the excited states [16]. It is known that YIG in the visible region has one CT transition at 490 nm and two crystal field (CF) type transitions at about 610 and 700 nm. The CT transition is responsible for a MO Kerr rotation in the visible region due to the large oscillator strength, while the CF transitions at 610 and 700 nm are irresponsible. This is because of the intra-3d transition nature having even parity of the CF transitions; owing to the parity forbidden character, the oscillator strength of the CF transitions is very weak. The oscillator strength is, however, enhanced when electric-dipole-allowed excitation, which can be admixed to relieve the parity constraint, lies close by in energy [14]. In the present study, the excited localized SPP in Au particles can be considered as an electric dipole. The excitation energy of the SPP lies close by that of the CF transitions of YIG. This may relieve the parity constraint and enhance the

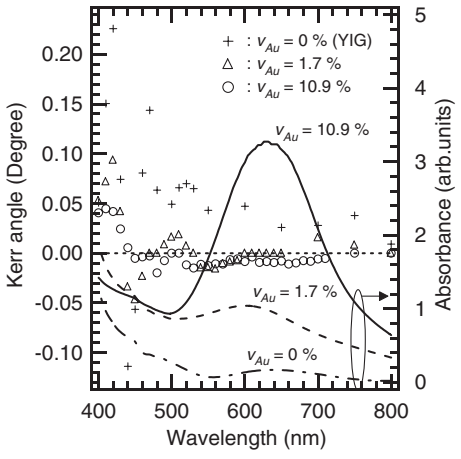

FIG. 3. Polar Kerr spectra for films with $v_{\mathrm{Au}} = 0\%$ (crosses), 1.7% (triangles), and 10.9% (circles). Absorption spectra in wavelength ranging from 400–800 nm are also shown for $v_{\mathrm{Au}} = 0\%$ (dash-dotted curve), 1.7% (dashed curve), and 10.9% (solid curve).

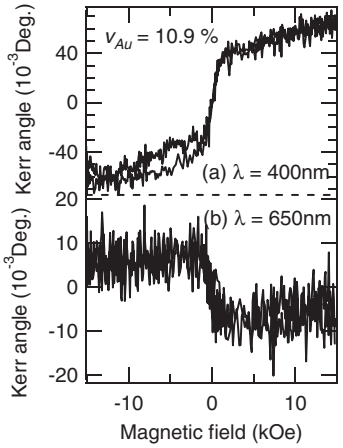

FIG. 4. Kerr loops of a film with $v_{\mathrm{Au}} = 10.9\%$ at wavelength of 400 nm (a) and 650 nm (b).

oscillator strength of the CF transitions, resulting in an anomalous Kerr rotation in the vicinity of 600 nm.

Furthermore, a modification of SO coupling of the excited states in the CT transition is possible. In a Bi substituted rare-earth iron garnet, the MO Faraday rotation angles in the visible region become negative with increasing Bi concentration [20,21]. The negative rotation was believed to be caused by the change of the sign of the SO coupling constants in the excited CT states in the iron garnet due to the substitution by Bi [16]. However, in the present study, the formation of an Au substituted YIG can be ruled out from the XRD study. The Hamiltonian of the SO coupling is described as $H_{\mathrm{SO}} = (\hbar/4mc^2)(\nabla V \times \vec{p}) \cdot \vec{\sigma}$, where V is the external potential, $\vec{p}$ is the momentum, and $\vec{\sigma}$ is the Pauli spin operator [22,23]. This equation indicates that the external electric potential V may influence the SO coupling in the magnetized materials. As already mentioned above, the electromagnetic energy concentration in the resonant state of the localized SPP causes a strong optical near-field around the nanoparticles even with modest input power. It is thus plausible that the localized SPP accompanied by an enhanced electric field modifies the sign of the effective SO coupling constant in the excited CT states of YIG in the vicinity of the interfaces with Au nanoparticles.

When we discuss the physics of the SPP of particles, we should take the particle size compared with the wavelength of light into consideration [17]. TEM studies showed that Au nanoparticles in the $v_{\mathrm{Au}} = 10.9\%$ sample is about 12 nm in average diameter. In the film with $v_{\mathrm{Au}} = 1.7\%$, the size is much smaller. Since the size of Au particles in both films is sufficiently small compared with the wavelength, in which the Kerr rotation angles change the sign and show negative values (500–700 nm), the retardation effects of light is negligible; the SPP wavelength of the particles is not affected by the particles size. Therefore, we think that a small variation in the Au particle diameter in this study does not influence the sign of the Kerr rotation.

It seems to be surprising that Au nanoparticles only about 10% at highest in volume fraction influence the MO properties of YIG matrices. This is primarily due to a large specific surface of the nanoparticles. The penetration length of the optical near-field by localized SPP is similar to the radius of the particle. The near field in the vicinity of the Au nanoparticles about 12 nm in diameter thus penetrates into YIG matrices about 6 nm in depth. Let us assume a simple three-dimensional arrangement of spherical Au particles 12 nm in diameter occupying the sites of a periodic cubic lattice in the film with a volume fraction of 10%, although Au particles in the actual samples are randomly dispersed. The surface-to-surface spacing between the nearest neighbor Au particles can be calculated to be about 8 nm. It is thus reasonable to think that the near-field contribution influences effectively the MO effect of YIG matrices in the $v_{\mathrm{Au}} = 10.9\%$ sample.

In conclusion, we have studied the MO Kerr effect of YIG thin films incorporating Au nanoparticles prepared using a cosputtering technique. TEM and XRD studies suggested that metallic Au nanoparticles are grown in the YIG matrices. UV-Vis transmission spectroscopy showed the localized SPP resonance of Au nanoparticles at about 600 nm. The polar MO Kerr spectra obtained at wavelengths ranging from 400 to 800 nm demonstrated that, by incorporating the Au nanoparticles, the Kerr rotation angles exhibit negative values in the vicinity of 600 nm. These results indicate a plausible coupling between the MO effect of YIG and the SPP through the near-field contribution. An enhancement of the oscillator strength of the CF transitions in YIG and a modification of effective SO coupling of YIG via the strong optical near field are possible mechanisms for the anomalous Kerr rotation. The present study suggests a possibility of controlling magnetic properties of nanocomposite magnetic materials via an optical near field.

The authors thank K. Shinagawa, C. Mitsumata, K. Akamatsu, K. Watanabe, D. Hashizume, and S. Ushioda for valuable discussions.

*Electronic address: s-tomita@riken.jp

[1] R. Ruppin, in *Electromagnetic Surface Modes*, edited by A. D. Boardman (Wiley, Chichester, 1982).
[2] S. Nie and S. R. Emory, Science **275**, 1102 (1997).
[3] S. A. Maier *et al.*, Nat. Mater. **2**, 229 (2003).
[4] X. Luoad and T. Ishihara, Appl. Phys. Lett. **84**, 4780 (2004).
[5] V. A. Kosobukin, Proc. SPIE Int. Soc. Opt. Eng. **2535**, 9 (1995).
[6] H. Feil and C. Haas, Phys. Rev. Lett. **58**, 65 (1987).
[7] T. Katayama *et al.*, Phys. Rev. Lett. **60**, 1426 (1988).
[8] V. I. Safarov *et al.*, Phys. Rev. Lett. **73**, 3584 (1994).
[9] C. Hermann *et al.*, Phys. Rev. B **64**, 235422 (2001).
[10] J. Bremer *et al.*, J. Appl. Phys. **89**, 6177 (2001).
[11] N. Bonod *et al.*, J. Opt. Soc. Am. B **21**, 791 (2004).
[12] T. J. Silva, S. Schultz, and D. Weller, Appl. Phys. Lett. **65**, 658 (1994).
[13] M. Abe and T. Suwa, Phys. Rev. B **70**, 235103 (2004).
[14] F. J. Kahn, P. S. Pershan, and J. P. Remeika, Phys. Rev. **186**, 891 (1969).
[15] S. Tomita *et al.*, J. Appl. Phys. **95**, 8194 (2004).
[16] K. Shinagawa, in *Magneto-Optics*, edited by S. Sugano and N. Kojima (Springer, Berlin, 1999).
[17] C. F. Bohren and D. R. Huffman, *Absorption and Scattering of Light by Small Particles* (Wiley, New York, 1983).
[18] E. D. Palik, *Handbook of Optical Constants of Solids* (Academic, New York, 1997).
[19] J. C. Maxwell-Garnet, Philos. Trans. R. Soc. London **203**, 385 (1904).
[20] H. Takeuchi, Jpn. J. Appl. Phys. **14**, 1903 (1975).
[21] Z. Šimša *et al.*, IEEE Trans. Magn. **20**, 1001 (1984).
[22] S. LaShell, B. A. McDougall, and E. Jensen, Phys. Rev. Lett. **77**, 3419 (1996).
[23] E. I. Rashba, Physica E (Amsterdam) **20**, 189 (2004), and references therein.